Tony Jourdan,[1] Gergő Szanda,[1] Resat Cinar,[1] Grzegorz Godlewski,[1] David J. Holovac,[1] Joshua K. Park,[1] Sarah Nicoloro,[2] Yuefei Shen,[2] Jie Liu,[1] Avi Z. Rosenberg,[3,4] Ziyi Liu,[1] Michael P. Czech,[2] and George Kunos[1]

Developmental Role of Macrophage Cannabinoid-1 Receptor Signaling in Type 2 Diabetes

Diabetes 2017;66:994–1007 | DOI: 10.2337/db16-1199

Islet inflammation promotes β-cell loss and type 2 diabetes (T2D), a process replicated in Zucker Diabetic Fatty (ZDF) rats in which β-cell loss has been linked to cannabinoid-1 receptor (CB_1R)–induced proinflammatory signaling in macrophages infiltrating pancreatic islets. Here, we analyzed CB_1R signaling in macrophages and its developmental role in T2D. ZDF rats with global deletion of CB_1R are protected from β-cell loss, hyperglycemia, and nephropathy that are present in ZDF littermates. Adoptive transfer of $CB_1R^{-/-}$ bone marrow to ZDF rats also prevents β-cell loss and hyperglycemia but not nephropathy. ZDF islets contain elevated levels of CB_1R, interleukin-1β, tumor necrosis factor-α, the chemokine CCL2, and interferon regulatory factor-5 (IRF5), a marker of inflammatory macrophage polarization. In primary cultured rodent and human macrophages, CB_1R activation increased *Irf5* expression, whereas knockdown of *Irf5* blunted CB_1R-induced secretion of inflammatory cytokines without affecting CCL2 expression, which was p38MAPKα dependent. Macrophage-specific in vivo knockdown of *Irf5* protected ZDF rats from β-cell loss and hyperglycemia. Thus, IRF5 is a crucial downstream mediator of diabetogenic CB_1R signaling in macrophages and a potential therapeutic target.

Obesity is a risk factor for insulin resistance (IR), which can lead to progressive dysfunction and loss of pancreatic β-cells resulting in overt type 2 diabetes (T2D) (1,2), although β-cell dysfunction may arise independently, as it can precede the onset of IR (3). Adipose tissue inflammation plays a critical role in obesity-related IR (4), and a similar process associated with inflammatory cell infiltration in the endocrine pancreas has been linked to β-cell loss and the development of T2D (5).

Endocannabinoids (ECs) are endogenous ligands of cannabinoid receptors (cannabinoid-1 receptor [CB_1R] and cannabinoid-2 receptor) that also mediate the effects of marijuana (6). The EC/CB_1R system is overactive in obesity/metabolic syndrome (7,8), and blockade or genetic deletion of CB_1R mitigates diet-induced obesity and its metabolic complications, including IR and T2D (reviewed by Mazier et al. [9]). CB_1R blockade has similar beneficial effects in people with metabolic syndrome (10) or T2D (11) but can cause psychiatric side effects due to blocking CB_1R in the central nervous system. ECs can inhibit hepatic insulin sensitivity via CB_1R in the central nervous system (12) but can also inhibit insulin signaling directly via CB_1R in adipose tissue (13), skeletal muscle (14), liver (15), and adipose tissue macrophages (16), and these latter targets account for the efficacy of peripherally restricted CB_1R antagonists in mitigating IR (17,18).

Macrophage CB_1Rs also play a prominent role in the progressive loss of β-cell function in Zucker Diabetic Fatty (ZDF) rats, a rodent model of T2D. The pancreatic islets of adult ZDF rats have reduced numbers of β-cells and are heavily infiltrated with proinflammatory macrophages expressing high levels of CB_1R and the Nlrp3/Asc inflammasome (19).

[1]Laboratory of Physiologic Studies, National Institute on Alcohol Abuse and Alcoholism, National Institutes of Health, Bethesda, MD
[2]Program in Molecular Medicine, University of Massachusetts Medical School, Worcester, MA
[3]Division of Renal Pathology, Department of Pathology, Johns Hopkins University, Baltimore, MD
[4]Kidney Diseases Section, National Institute on Diabetes and Digestive and Kidney Diseases, National Institutes of Health, Bethesda, MD

Corresponding author: Tony Jourdan, tony.jourdan@nih.gov, or George Kunos, george.kunos@nih.gov.

Received 7 October 2016 and accepted 8 January 2017.

This article contains Supplementary Data online at http://diabetes.diabetesjournals.org/lookup/suppl/doi:10.2337/db16-1199/-/DC1.

T.J. and G.S. contributed equally to this work.

G.S. is currently affiliated with the Department of Physiology, Faculty of Medicine, Semmelweis University, Budapest, Hungary.

Peripheral CB_1R blockade, macrophage depletion, or macrophage-specific knockdown of CB_1R prevented these changes and preserved normoglycemia (19), which further illustrates the anti-inflammatory effect of CB_1R blockade. Chronic CB_1R blockade promotes a shift in the polarization of macrophages from proinflammatory to anti-inflammatory (19) and also reduces macrophage infiltration of diabetic islets by inhibiting the secretion of MCP-1 (or CCL2) (19,20). ZDF rats also develop severe diabetic nephropathy associated with a loss of glomerular podocytes without significant macrophage infiltration or increase in Nlrp3/ASC inflammasome expression in the kidney (21).

Together, these findings raise questions of whether there is an obligatory role for ECs in the development of T2D and its renal complication in the ZDF model. To this end, we have generated CB_1R-deficient rats on a ZDF background (ZDF-Cnr1 rats) and analyzed glycemic functions and renal parameters, as well as their modulation by adoptive bone marrow (BM) transfer. Our results indicate the obligatory requirement for peripheral CB_1Rs in both T2D and diabetic nephropathy, with CB_1R in BM-derived cells required for β-cell loss and the development of hyperglycemia, but not for podocyte loss and the resulting nephropathy.

Interferon regulatory factor-5 (IRF5) was recently implicated in polarizing macrophages toward the inflammatory phenotype (22), whereas mice with global or macrophage-specific deletion of *Irf5* that were maintained on a high-fat diet remain insulin sensitive and display beneficial expansion of subcutaneous adipose tissue (23). Because of the unexpected similar expansion of subcutaneous but not visceral fat tissue observed in ZDF-Cnr1 rats, we explored the involvement of IRF5 in β-cell loss via CB_1R-mediated inflammatory signaling. Here we report that IRF5 mediates CB_1R-induced cytokine secretion and the resulting β-cell loss, whereas CB_1R-induced CCL2 production and macrophage transmigration is independent of IRF5 and involves activation of the α-isoform of p38 mitogen-activated protein kinase (p38MAPK).

RESEARCH DESIGN AND METHODS

Animals

Animal protocols were approved by our institutional animal care and use committee. Male ZDF rats and their lean controls were obtained from Charles River Laboratories, housed individually under a 12-h light/dark cycle, and fed ad libitum a standard laboratory diet (STD; NIH-31 Rodent Diet).

Generation and Characterization of ZDF-Cnr1 Rats

A pair of zinc finger nucleases (Sigma-Aldrich, St. Louis, MO) was designed to cleave within the coding region of the *Cnr1* gene, with the target site 5′-TACCACTTC ATCGGCAGCctggcaGTGGCCGACCTCCTG-3′ (zinc finger nuclease binding site set in capital letters). Identified founders carried an 11–base pair (BP) deletion located between T^{17193} to C^{17203} in the genomic DNA sequence.

Genotyping

Cnr1 and *Fa* genes were amplified as described in Supplementary Table 2.

Drugs and Chemicals

JD5037 was synthesized and its pharmacological properties analyzed as described previously (18). CP-55,940 was obtained from the NIDA Drug Supply Program (Research Triangle Park, NC). *N*-arachidonoylethanolamine (or anandamide [AEA]), arachidonoyl-2′-chloroethylamine (ACEA) and SP600125 were purchased from Cayman (Ann Arbor, MI). SB202190 was from Calbiochem (La Jolla, CA). All other chemicals were from Sigma-Aldrich.

Serum and Urine Parameters

Blood glucose levels were determined using the Elite Glucometer (Bayer, Pittsburgh, PA). Serum alanine aminotransferase (ALT), aspartate aminotransferase, free fatty acid (FFA), total cholesterol, triglycerides, insulin, proinsulin, C-peptide, glucagon, leptin, and adiponectin were quantified as described previously (19). IGF-I content was quantified with a Mouse/Rat IGF-I ELISA Kit (R&D Systems, Minneapolis, MN), whereas growth hormone was detected using a Rat/Mouse ELISA Kit (Millipore, Billerica, MA). Serum and urine creatinine, urea, and albumin concentrations and glomerular filtration rate were determined as described previously (21).

Glucose Tolerance, Insulin Sensitivity Tests, HOMA-IR, and Glucose-Stimulated Insulin Secretion

Glucose tolerance and insulin sensitivity tests were performed as described previously (24). HOMA-IR was calculated as follows: fasting insulin (μU/mL) × fasting glucose (mg/dL)/405 (25). Glucose-stimulated insulin secretion (GSIS) was determined as described previously (19).

GTPγS Binding

[^{35}S]GTPγS binding assay was performed as described (26).

Whole-Body Irradiation and BM Transfer

Whole-body irradiation was conducted as described previously (27). Six-week-old male ZDF rats received 1 Gy total body irradiation from a ^{137}Cs source. BM cells from ZDF and ZDF-Cnr1 donor rats were obtained as described previously (27). After a 2-h rest after irradiation, recipient rats were injected with 10^8 BM cells via a tail vein. Animals were then rested for 2 weeks, and survivors with proper chimerism were used for experiments.

Determination of Chimerism

DNA was isolated from blood using a DNeasy kit (69504; Qiagen, Germantown, MD). *Cnr1* expression was detected using the genotyping protocol.

Blood Cell Counts

Blood samples were analyzed in an automated Hemavet blood analyzer (Drew Scientific Group, Miami Lakes, FL).

Histology and Immunohistochemistry

Pancreas, kidney, and adipose tissue were fixed in 10% neutral buffered formalin, embedded in paraffin, and sectioned (4-μm sections) onto glass slides. Renal and adipose tissue histology were evaluated after hematoxylin-eosin and periodic acid Schiff staining. The antibodies used are listed in

Supplementary Table 3. Slides were revealed by using the appropriate Elite ABC HRP (horseradish peroxidase)/diaminobenzediene (DAB) system (Vector Laboratories), counterstained with hematoxylin-eosin (Gills Formula; Vector Laboratories), or by secondary antibodies coupled to Alexa Fluor 488, 555, or 647. DAB slides were analyzed using an Olympus BX41 microscope, whereas fluorescent staining was analyzed using a Zeiss LSM700 confocal microscope. Immunopositivity was quantified using ImageJ software. Adipocyte diameters were evaluated digitally in light microscopy images of adipose tissue sections (n = 6–7 pictures per animal, three animals per group) using ImageJ software.

TUNEL Staining

TUNEL staining in pancreatic islet was performed using the Click-it TUNEL Alexa Fluor Imaging Assay from ThermoFisher Scientific (C10245).

Isolation of Pancreatic Islets, β-Cell Mass

Islets were isolated, and β-cell mass was determined as described previously (19).

Islets Inflammation

Caspase-1 activity was determined using the Caspase-1 Assay Kit (Fluorometric) from Abcam (ab39412); interleukin (IL)-1β and tumor necrosis factor-α (TNF-α) proteins were measured using the Rat Quantikine ELISA Kit (R&D Systems).

Cell Culture

Human monocytic THP-1 cells were grown according to the recommendation of the American Type Culture Collection (ATCC). Cells were differentiated at 1.5–2 $\times$ 10^6 cells/well (35 mm) with 50 ng/mL phorbol myristic acid (P8139; Sigma-Aldrich) for 4 days. THP-1–derived macrophages were incubated in RPMI 1640 free of phorbol myristic acid, supplemented with 10% FBS (30–2020; ATCC), 50 μg/mL streptomycin, and 50 units/mL penicillin (30–2300; ATCC) for 24 h at 37°C, under an atmosphere of 5% CO_2 in air prior to treatment. IL-1β, IL-18, IL-6, CCL2, and TNF-α protein concentrations were determined using ELISA kits from R&D Systems according to the manufacturer protocol.

Small Interfering RNA Gene Knockdown

Aliquots of peritoneally elicited macrophages (PEC) or THP-1 cells were exposed for 48 h to siRNA listed in Supplementary Table 4. Control siRNAs were designed using the C911 technique (28).

Preparation and In Vivo Administration of Glucan-Encapsulated siRNA Particles

Fluorescein isothiocyanate–labeled glucan shells were prepared as described previously (29), and 8-week-old ZDF rats were then injected intraperitoneally every other day for 12 days with 6.17 mg/kg glucan-encapsulated siRNA particles (GeRPs) loaded with 308 nmol/kg endoporter and 0.410 mg/kg siRNA (Supplementary Table 4).

Immunoblotting

Cells were treated with pertussis toxin (PTX) 100 ng/mL, SB202190 25 μmol/L, SP600125 25 μmol/L, JD5037 100 nmol/L, and AEA and ACEA 1–10 μmol/L. Western blotting analyses were conducted as described previously (30), and antibodies used are listed in Supplementary Table 5.

Real-Time PCR

Total RNA extraction, reverse transcription, and real-time PCR were performed as described previously (19).

Statistics

If not otherwise specified, values are expressed as the mean ± SEM. Data were analyzed by Student t test or by one-way ANOVA followed by the Tukey-Kramer post hoc test. Time-dependent variables were analyzed, and results in multiple groups were compared by two-way ANOVA followed by Bonferroni test. Significance was set at $P < 0.05$.

RESULTS

Generation and Characterization of *Cnr1*$^{-/-}$ Rats on a ZDF Background

ZDF rats with a global knockout of CB_1R (ZDF-Cnr1 rats) retained the mutation of the leptin receptor gene characteristic of Zucker fatty rats and ZDF rats and had an 11-BP deletion in the *Cnr1* genomic DNA, as demonstrated by genotyping (Fig. 1*A*). Of note, the *Cnr1* mutation led to a frameshift in the open reading frame resulting in a premature stop codon. As a result, CB_1R protein was undetectable in the brain of ZDF-Cnr1 rats (Fig. 1*B*). In addition, the CB_1R agonist CP-55940 increased [^{35}S]GTPγS binding in plasma membranes prepared from ZDF but not from ZDF-Cnr1 brains (Fig. 1*C*), confirming the absence of CB_1R signaling in the knockouts. ZDF-Cnr1 rats displayed lower food intake throughout the observation period and a slower rate of weight gain compared with their ZDF littermates but reached a similar body weight by the age of 26 weeks (Fig. 1*D*). Interestingly, the inguinal fat mass (often referred to as subcutaneous fat) was significantly larger in ZDF-Cnr1 than in ZDF rats, whereas the epididymal and perirenal fat pads, representing visceral fat, were of similar size (Fig. 1*E*). This was associated with a striking increase in the diameter of inguinal adipocytes in ZDF-Cnr1 versus ZDF rats, whereas an analogous difference in the size of perirenal adipocytes was much smaller (Supplementary Fig. 1).

The elevated serum levels of ALT, triglycerides, FFAs, and total cholesterol in ZDF rats were normalized in ZDF-Cnr1 rats (Fig. 1*F*). Additionally, the absence of *Cnr1* resulted in normalization of the reduced plasma levels of growth hormone and IGF-I observed in ZDF rats (Fig. 1*G*). The hypoadiponectinemia of ZDF rats was reversed beyond the levels in lean controls, whereas the hyperleptinemia was unaffected by the deletion of *Cnr1* (Fig. 1*G*).

β-Cell Function Is Preserved and Hyperglycemia Prevented by *Cnr1* Deletion

ZDF rats develop extreme hyperglycemia due to β-cell loss by the age of 12–14 weeks (19). In contrast, ZDF-Cnr1 rats remained euglycemic for up to 26 weeks of age (Fig. 2*A*). At 8 weeks (i.e., before hyperglycemia starts to develop in ZDF

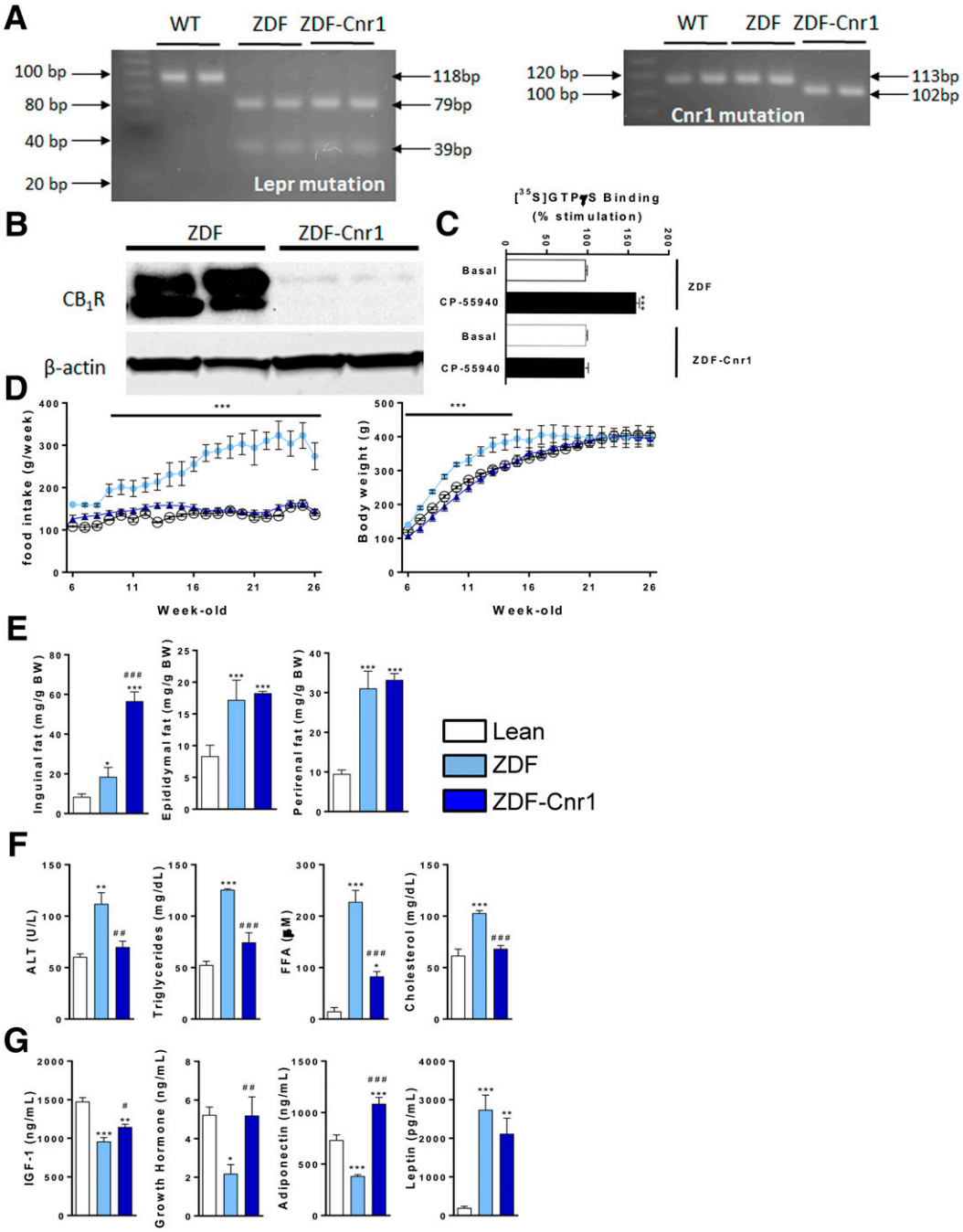

Figure 1—Characterization of ZDF-Cnr1 rats. *A*: Representative gel analysis for *Lepr* mutation and *Cnr1* mutation. *B*: CB_1R immunoblot from a ZDF vs. ZDF-Cnr1 brain. *C*: [^{35}S]GTPγS binding assay using membranes from ZDF vs. ZDF-Cnr1 brains; columns and bars represent the mean ± SEM from five separate preparations. ***$P < 0.005$ relative basal activity. *D*: Daily food intake and body weight measurements from 6 to 26 weeks of age in lean controls, ZDF rats, and ZDF-Cnr1 rats. Points and bars represent the mean ± SEM from lean control (open circles), ZDF (light blue circles), and ZDF-Cnr1 (blue triangles) rats. *E*: Weight of inguinal, epididymal, and perirenal fat pads in lean (open columns, $n = 10$), ZDF (light blue, $n = 10$), and ZDF-Cnr1 rats (blue, $n = 10$). *F*: Serum ALT, triglyceride, FFA, and total cholesterol levels. *G*: Serum concentration of IGF-I, growth hormone, adiponectin, and leptin levels. Columns and bars represent the mean ± SEM. Significant differences from values in lean controls (*) or ZDF rats (#), * or #$P < 0.05$, ** or ##$P < 0.01$, *** or ###$P < 0.001$. BW, body weight; WT, wild type.

rats), ZDF-Cnr1 rats were more glucose tolerant than ZDF rats (Fig. 2*B*). In contrast, the two strains displayed equal IR in the insulin sensitivity test (Fig. 2*C*), as is also reflected by the similar degree of hyperinsulinemia and similar increases in HOMA-IR (Fig. 2*D*). Despite their similar IR, ZDF-Cnr1 rats have improved β-cell function, as reflected in the preserved GSIS, whereas ZDF rats were nonresponsive to a glucose challenge (Fig. 2*E*).

ZDF-Cnr1 rats exhibited normal plasma levels of glucagon in contrast to the hyperglucagonemia of ZDF

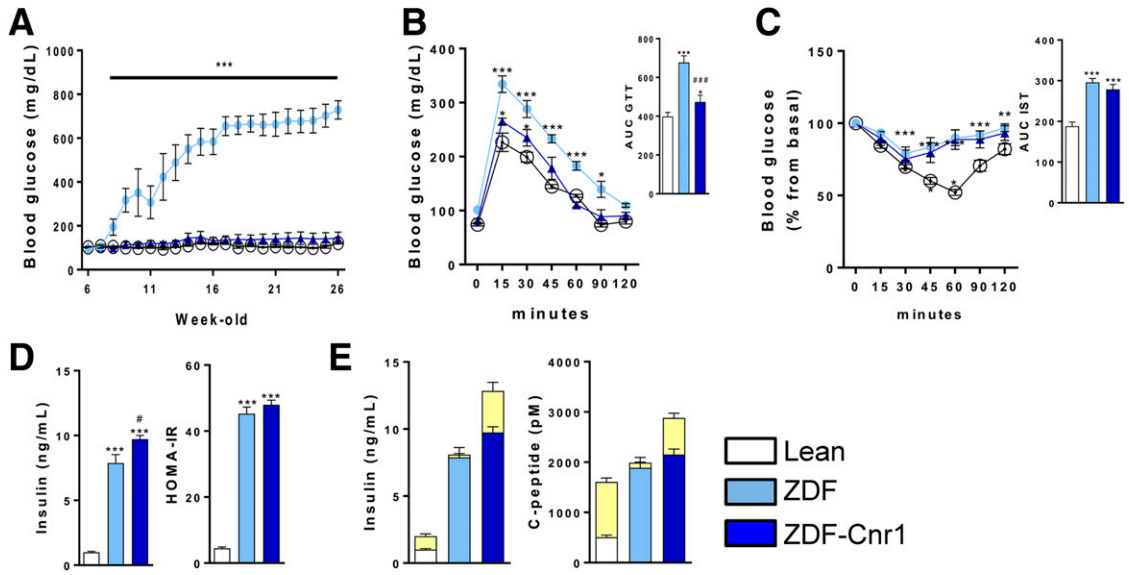

Figure 2—Glycemic control and β-cell status in lean control, ZDF, and ZDF-Cnr1 rats. *A*: Evolution of blood glucose from 6 to 26 weeks of age in lean (open circles), ZDF (light blue circles), and ZDF-Cnr1 (blue triangles) rats. *B*: Glucose tolerance tests conducted at 8 weeks of age, as described in RESEARCH DESIGN AND METHODS. *C*: Insulin sensitivity tests (ISTs) at 8 weeks, as described in RESEARCH AND DESIGN METHODS. *D*: Serum insulin and HOMA-IR at 8 weeks. *E*: GSIS indicated by the yellow segments, determined at 8 weeks, as described in RESEARCH DESIGN AND METHODS. Columns and bars represent mean ± SEM (n = 8–10 rats/group). Significant difference from corresponding value in lean (white bars) (*P < 0.05, **P < 0.01, ***P < 0.001) or ZDF rats (light blue bars) (#P < 0.05, ###P < 0.001). AUC, area under the curve.

rats (Fig. 3*A*), which may contribute to the improved glucose tolerance in the presence of IR in ZDF-Cnr1 rats. Also, plasma proinsulin, insulin, and C-peptide levels were higher whereas the proinsulin/insulin ratio was significantly lower in ZDF-Cnr1 than in ZDF littermates (Fig. 3*A*), which is indicative of improved β-cell function and survival. The protection of β-cells in ZDF-Cnr1 rats was further confirmed by the higher islet insulin content (Fig. 3*B*). Of note, the strong infiltration of islets with $CD68^+$ macrophages previously observed in younger, 14-week-old ZDF rats (19) was absent by the age of 26 weeks (Fig. 3*B*), probably due to the nearly complete destruction of islets by this age. Nevertheless, in a few remaining identifiable islets we could still observe strong infiltration of $CD68^+$ macrophages (Fig. 3*B*, third row). In contrast, ZDF-Cnr1 rats maintained an almost normal islet structure without prominent $CD68^+$ macrophage infiltration and had significantly larger β-cell mass than ZDF littermates (Fig. 3*C*). The higher β-cell mass inversely correlated with β-cell death, as reflected by the increased number of TUNEL-positive cells in ZDF compared with ZDF-Cnr1 islets (Supplementary Fig. 2*A*).

ZDF-Cnr1 Rats Are Protected From Diabetic Nephropathy

CB_1R is a major effector in the development of diabetic nephropathy, and treatment of ZDF rats with a peripheral CB_1R antagonist prevented or reversed this complication (21). Diabetic nephropathy, evident in 26-week-old ZDF rats by robust deterioration in renal parameters, was largely absent in ZDF-Cnr1 rats, as reflected in normalization of the albuminuria, glomerular filtration rate, and blood urea nitrogen (Supplementary Fig. 3*A*). Correspondingly, ZDF-Cnr1 rats were protected from podocyte loss, as demonstrated by Wilms tumor 1 immunostaining (Supplementary Fig. 3*B*). Furthermore, ZDF rats displayed glomerular enlargement and early mesangial matrix expansion that were absent in lean control or ZDF-Cnr1 rats. The pronounced albuminuria of ZDF rats was associated with prominent tubular protein resorption droplets and occasional tubular dilatation with proteinaceous casts. Again, no such changes were observed in ZDF-Cnr1 rats (Supplementary Fig. 3*C*).

CB_1R in Myeloid Cells Drive β-Cell Loss and Hyperglycemia but Not Nephropathy or Dyslipidemia

Since macrophages are derived from BM myeloid precursors, we used the irradiation-BM transplantation (BMT) approach to test whether the lifelong β-cell protection in ZDF-Cnr1 rats is due to the absence of CB_1R in macrophages.

For total body radiation exposure from a ^{137}Cs source, 1 Gy was the dose high enough to eliminate all circulating white blood cells without being lethal for at least 7 days after irradiation (Supplementary Fig. 4). Also, recipient rats needed at least 10^8 donor BM cells to ensure survival. Animals were therefore irradiated at 6 weeks of age and transplanted 2 h after irradiation with 10^8 BM cells pooled from three donor animals. Two weeks later, white blood cells were collected and DNA was extracted to verify the donor genotype. Five of seven recipients survived in each group, with all survivors achieving the expected chimerism (Fig. 4*A*).

BMT from ZDF donors to ZDF recipients tested for genotype-independent effects of irradiation and BMT. Recipients developed progressive hyperglycemia from 14 weeks on, reaching a plateau at 600 mg/dL by week

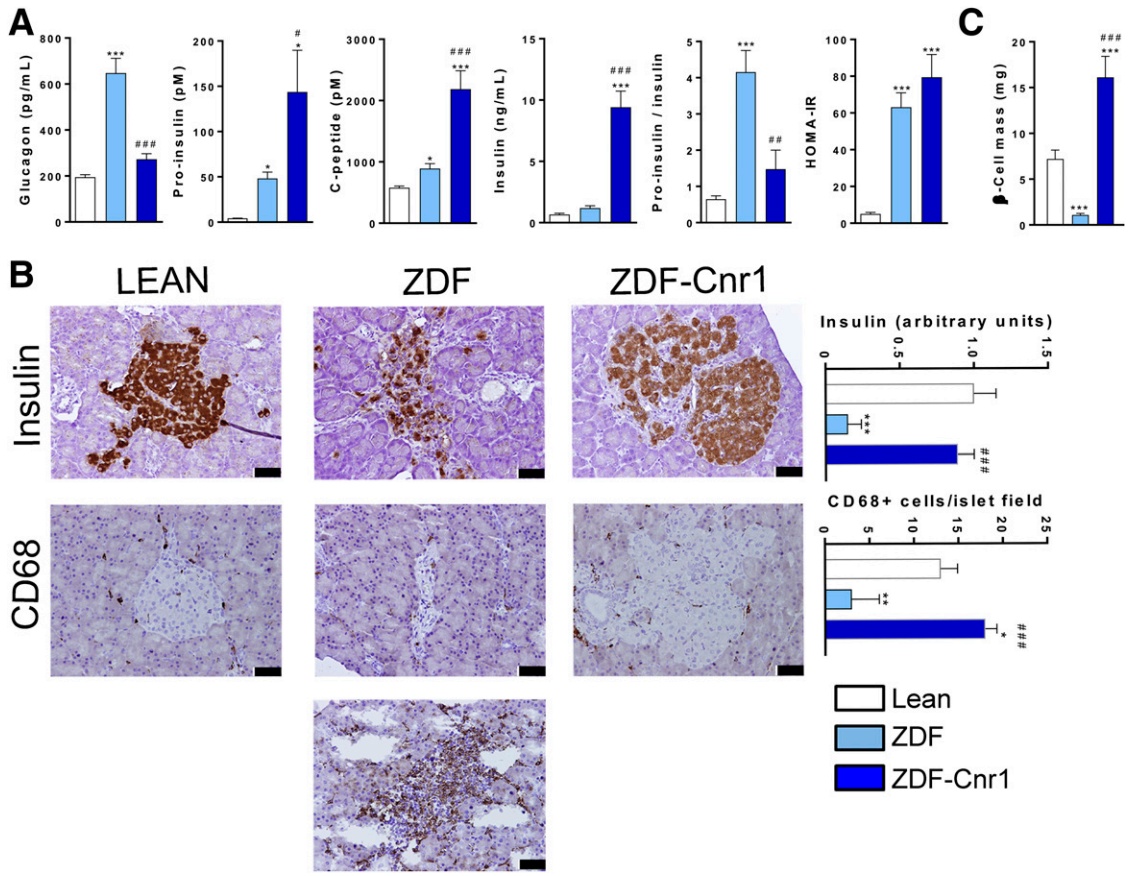

Figure 3—Hormonal parameters and β-cell status in lean, ZDF, and ZDF-Cnr1 rats. *A*: Serum hormone levels, proinsulin/insulin ratio, and HOMA-IR, determined at 26 weeks of age in lean (open), ZDF (light blue), and ZDF-Cnr1 rats (blue). *B*: Islet insulin and CD68$^+$ cell content determined by immunohistochemistry after killing of the rats at 26 weeks. The bottom (seventh) panel illustrates a rare remaining islet heavily infiltrated by CD68$^+$ cells. *C*: β-Cell mass, determined as described in RESEARCH DESIGN AND METHODS. Columns and bars are the mean ± SEM from 8–12 animals/group. Scale bar, 100 μm. $^*P < 0.05$, $^{**}P < 0.01$, $^{***}P < 0.001$ compared to lean control; #$P < 0.05$, ##$P < 0.01$, ###$P < 0.001$ compared to ZDF rats.

20 (Fig. 4*B*). The extent and rate of development of hyperglycemia were similar to those in control ZDF rats (dashed line), but its onset was delayed by 6 weeks, corresponding to the time it takes for the transferred cells to repopulate the irradiated BM and peripheral tissues (27). In contrast, ZDF rats receiving BM from ZDF-Cnr1 donors remained normoglycemic throughout the entire 20-week observation period and maintained higher plasma insulin and C-peptide levels compared with rats receiving ZDF BM (Fig. 4*B*). Interestingly, there was no difference in food intake or body weight between the two groups (Fig. 4*B*). CB_1R protein was readily detectable postmortem in the BM of recipients of ZDF BM but was absent in recipients of ZDF-Cnr1 BM. As expected, CB_1R was present at similar high levels in brain samples from both groups (Fig. 4*C*). Furthermore, CB_1R highly colocalized with CD68$^+$ macrophages in the islets of ZDF rats transplanted with ZDF BM, whereas there were fewer CD68$^+$ cells and no detectable CB_1Rs in islets of recipients of ZDF-Cnr1 BM (Fig. 4*D*). The absence of CB_1Rs in hematopoietic cells was associated with higher pancreatic insulin content, normal pancreatic islet architecture, and reduced CD68$^+$ macrophage infiltration, most likely due to reduced levels of the chemoattractant protein CCL2 (Fig. 4*E*). β-Cells in ZDF islets produce CCL2 (31,32) (Supplementary Fig. 2*B*), whereas the dramatically higher CCL2 expression in islets of ZDF rats transplanted with wild-type compared with *Cnr1*$^{-/-}$ BM (Fig. 4*E*) suggests that transmigrating macrophages contribute to CCL2 secretion, as also supported by the ability of cultured macrophages to secrete CCL2 (see below) (Figs. 5 and 6).

In contrast, adoptive transfer of *Cnr1*$^{-/-}$ BM did not influence the dyslipidemia (Supplementary Table 2) or the development of diabetic nephropathy (Supplementary Fig. 5*A*), including the loss of Wilms tumor 1–positive podocytes (Supplementary Fig. 5*B*).

Distinct CB_1R Signaling Pathways Involved in Chemokine and Inflammatory Cytokine Secretion by Macrophages

Next, we analyzed the CB_1R signaling pathways that mediate the diabetogenic functions of macrophages (19). The

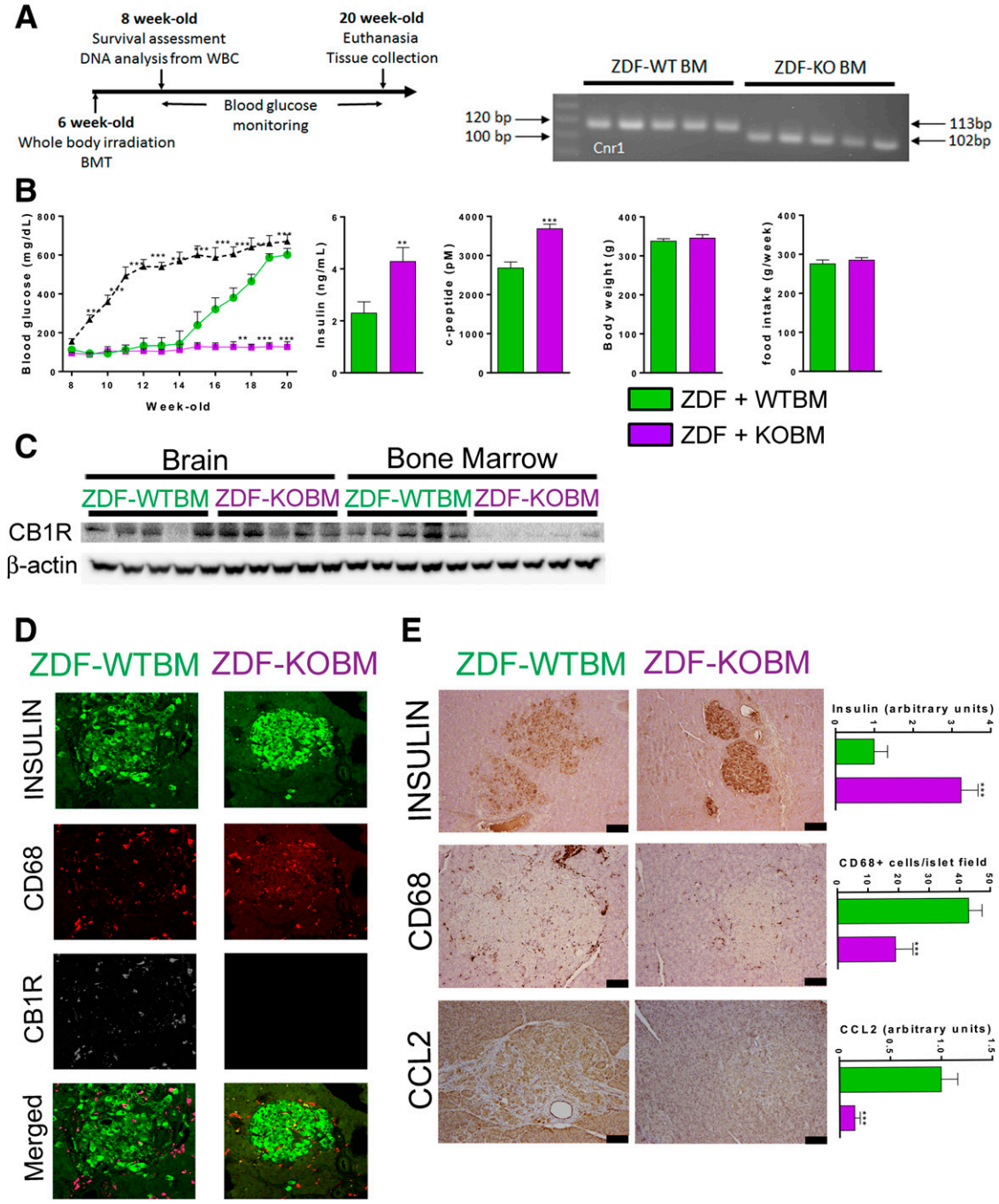

Figure 4—CB_1R ablation in myeloid cells protects ZDF rats from hyperglycemia. *A*: Time line for whole-body irradiation/BM transfer; genotyping by agarose gel chromatography of white blood cells (WBCs) from ZDF rats receiving ZDF BM (WTBM) or ZDF-KO BM (KOBM), with the 113-BP and 102-BP amplicons indicating *Cnr1*$^{+/+}$ and *Cnr1*$^{-/-}$ genotype, respectively. *B*: Evolution of blood glucose and serum levels of insulin and C-peptide along with body weight and mean weekly food intake at 20 weeks in ZDF rats receiving wild-type BM (green) or *Cnr1*$^{-/-}$ BM (purple). Filled triangles and the dashed line indicates blood glucose levels in nonirradiated ZDF rats. *C*: Western blot of CB_1R protein in brain and BM cells after killing of the rats at 20 weeks. *D*: Fluorescence immunohistochemistry of insulin, CB_1Rs, CD68, and colocalization analyzed by confocal microscopy. *E*: Increased insulin and decreased CD68 and CCL2 content of islets from ZDF rats receiving *Cnr1*$^{-/-}$ compared with wild-type ZDF BM. Columns and bars are the mean ± SEM from $n = 5$ animals/group. Scale bar, 100 μm. $^{**}P < 0.01$, $^{***}P < 0.001$ relative to values in ZDF rats receiving wild-type BM (green columns).

stimulation of rat PECs with the physiological CB_1R agonist AEA (5 μmol/L) or its stable analog ACEA (5 μmol/L) activated p38MAPK and c-Jun N-terminal kinase (JNK) 2 without any detectable change in extracellular signal–regulated kinase 1/2 (ERK1/2) phosphorylation (Fig. 5*A*). CB_1R activation reduced STAT3 phosphorylation, a known corollary of M1 polarization (33), which was inversely related to p38MAPK activation (Fig. 5*A*). ACEA also induced the

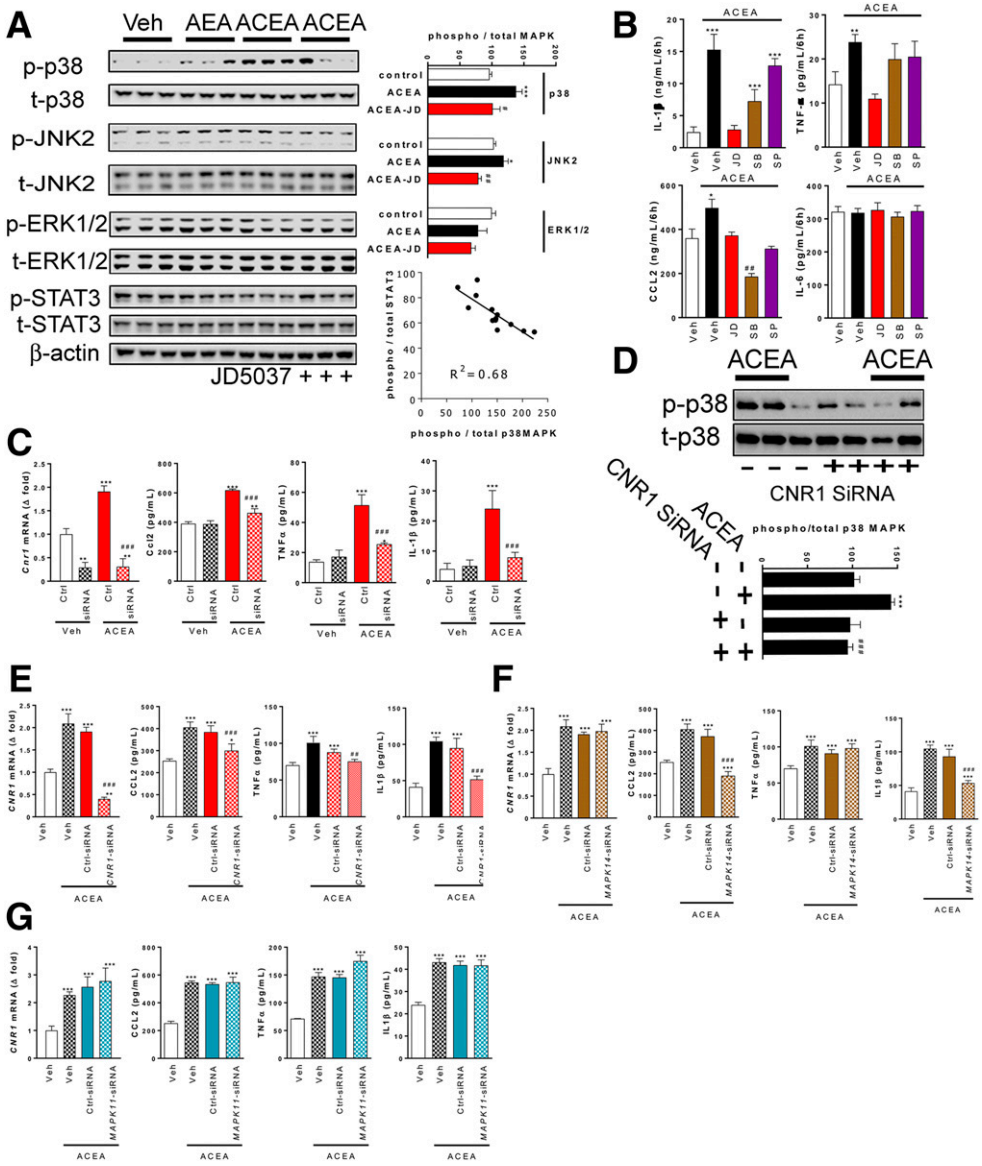

Figure 5—Role of MAP kinases in CB_1R-induced chemokine and cytokine secretion by rat peritoneal macrophages (*A–D*) or THP-1 cells (*E–G*). *A*: Western blot analysis of phosphorylation of p38MAPK, JNK2, or ERK1/2 by 5 μmol/L AEA or 5 μmol/L ACEA in the presence or absence of 100 nmol/L JD5037 in three representative experiments; quantitation by densitometry. Bottom right: inverse relationship between ACEA-induced phosphorylation of p38MAPK and STAT3. *B*: Chemokine (CCL2) and cytokine secretion by 10^6 cells/well over 8 h in the presence of the indicated drugs. *C*: Effects of *Cnr1* siRNA knockdown on *Cnr1* mRNA and on chemokine and cytokine secretion induced by 5 μmol/L ACEA by aliquots of 10^6 rat peritoneal macrophages. *D*: siRNA-mediated knockdown of *Cnr1* inhibits ACEA-induced p38MAPK phosphorylation. *E*: Experiments as in *C*, using human THP-1 cells. *F*: Effects of p38MAPKα knockdown on ACEA-induced chemokine and cytokine secretion by THP-1 cells. *G*: Effects of p38MAPKβ knockdown on the same parameters. $^*P < 0.05$, $^{**}P < 0.01$, $^{***}P < 0.001$ relative to vehicle; $\#P < 0.05$, $\#\#P < 0.01$, $\#\#\#P < 0.001$ relative to ACEA-treated cells. Columns and bars are the mean ± SEM from four independent experiments. Ctrl, control.

secretion of the cytokines IL-1β and TNF-α and the chemokine CCL2, but failed to affect IL-6 production (Fig. 5*B*). SB202190, a potent inhibitor of p38MAPKα and p38MAPKβ, suppressed the secretion of CCL2 below control levels but did not affect TNF-α secretion, and a partial reduction of CB_1R-evoked IL-1β secretion was not statistically significant (Fig. 5*B*). The JNK1/2/3 inhibitor SP600125, while fully abolishing c-Jun phosphorylation (data not shown), was only effective in inhibiting the ACEA-evoked CCL2 secretion (Fig. 5*B*). The effects of ACEA on PEC secretory responses were fully abolished by the CB_1R inverse agonist JD5037 (Fig. 5*B*) and were similarly inhibited by siRNA-mediated selective knockdown of *Cnr1* (Fig. 5*C*).

In the macrophage-differentiated human monocytic cell line THP-1, silencing *CNR1* abolished ACEA-induced p38MAPK activation (Fig. 5*D*) and TNF-α, IL-1β, and CCL2 secretion (Fig. 5*E*). Knocking down *MAPK14* (encoding p38MAPKα), but not *MAPK11* (encoding p38MAPKβ),

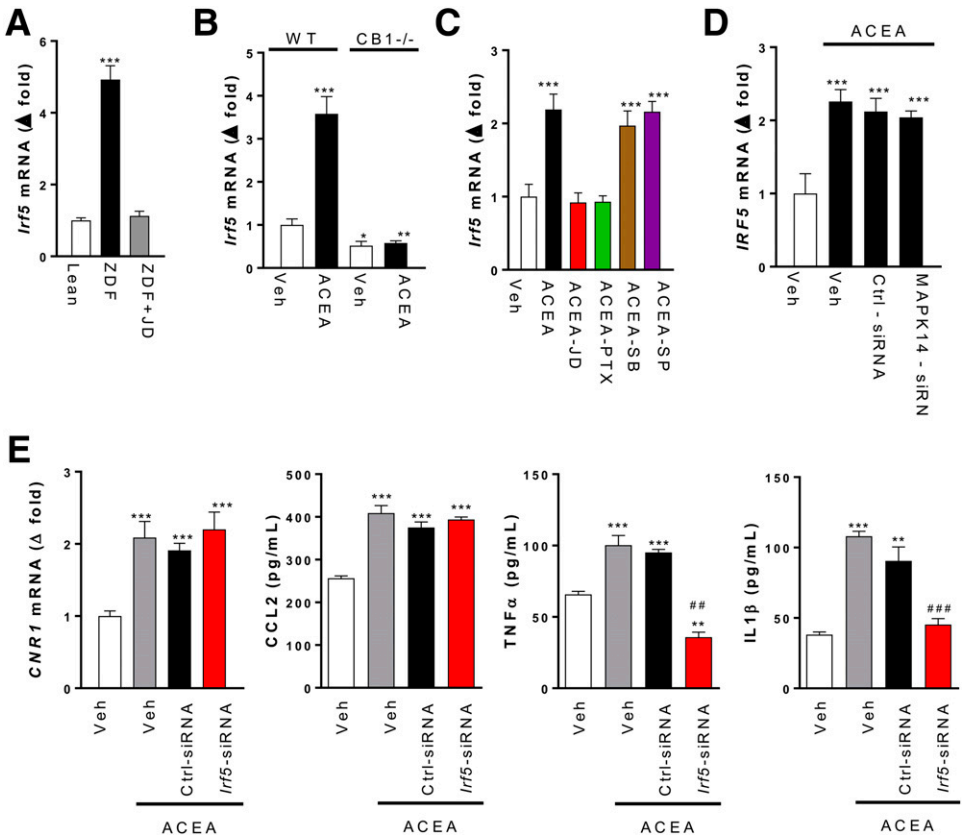

Figure 6—CB_1R regulation of *Irf5* expression and its role in β-cell loss in vivo. *A*: *Irf5* mRNA levels in islets isolated from lean control (Ctrl) and ZDF rats treated for 4 weeks with vehicle (Veh) or 3 mg/kg/day JD5037. *B*: *Irf5* mRNA levels in PECs isolated from wild-type or *Cnr1*$^{-/-}$ mice exposed to vehicle or 5 μmol/L ACEA for 24 h. *C*: *Irf5* mRNA in rat PECs treated with vehicle or 5 μmol/L ACEA alone or in the presence of 100 nmol/L JD5037, 100 ng/mL PTX, 25 μg/mL SB202190, or 25 μg/mL SP600125. *D*: ACEA-induced increase in *IRF5* expression is not affected by *MAPK14* knockdown. *E*: Effects of *Irf5* knockdown on *Cnr1* mRNA and on chemokine and cytokine secretion induced by 5 μmol/L ACEA in aliquots of 10^6 rat peritoneal macrophages. Points/columns and bars are the mean ± SEM from six rats/group. Significant differences from values in Veh (*) or Veh + ACEA groups (#). *$P < 0.05$; **$P < 0.01$; ***$P < 0.001$; ##$P < 0.01$; ###$P < 0.001$.

completely blocked ACEA-induced secretion of CCL2 and significantly reduced the secretion of IL-1β but, again, failed to influence ACEA-induced TNF-α secretion (Fig. 5*F* and *G*). Thus, CB_1R activation in macrophages engages p38MAPKα to induce CCL2, but not TNF-α, secretion and partially contributes to IL-1β secretion.

Prompted by the similar selective expansion of subcutaneous, but not visceral, fat tissue in ZDF-Cnr1 rats (Fig. 1*E*) and in mice deficient in the proinflammatory transcription factor Irf5 (see Introduction), we explored the involvement of IRF5 in CB_1R-mediated inflammatory signaling and β-cell loss. *Irf5* gene expression was robustly increased in pancreatic islets isolated from ZDF compared with lean rats, whereas there was no such increase in islets of ZDF-Cnr1 rats or in islets of ZDF rats chronically treated with JD5037 (Fig. 6*A*). The involvement of CB_1R was further confirmed in PECs isolated from wild-type mice, exposure of which to 1 μmol/L ACEA induced a threefold to fourfold increase in *Irf5* mRNA, with no such effect in PECs from *Cnr1*$^{-/-}$ mice (Fig. 6*B*). Furthermore, in rat PECs, 1 μmol/L ACEA increased *Irf5* mRNA twofold, an effect blocked by JD5037 or PTX but not by SB202190 or SP600125 (Fig. 6*C*). Thus, CB_1R regulates *Irf5* expression via $G_{i/o}$-mediated inhibition of adenylate cyclase rather than activation of MAP kinases. In THP-1 macrophages, 1 μmol/L ACEA also caused an approximately twofold increase in *IRF5* mRNA, and a similar effect was seen in THP-1 cells with siRNA-mediated knockdown of *MAPK14*, confirming the lack of involvement of p38MAPKα (Fig. 6*D*). SiRNA-mediated knockdown of *Irf5* in rat PECs inhibited the ACEA-induced secretion of both TNF-α and IL-1β but had no effect on CCL2 secretion or *Cnr1* expression (Fig. 6*E*), suggesting a requirement for IRF5 in CB_1R-mediated cytokine production.

To explore the potential role of the $CB_1R/G_{i/o}$/IRF5 signaling cascade in the loss of β-cell function in ZDF rats, 8-week-old ZDF rats were chronically treated with GeRP containing siRNA against rat *Irf5*, a technique that allows selective knockdown of target genes in phagocytic macrophages in vivo (19,34). We first optimized *Irf5* siRNAs and selected one that yielded >90% knockdown of *Irf5* gene expression in rat PECs after 48 h (Fig. 7*A*). ZDF rats were then treated intraperitoneally every other day

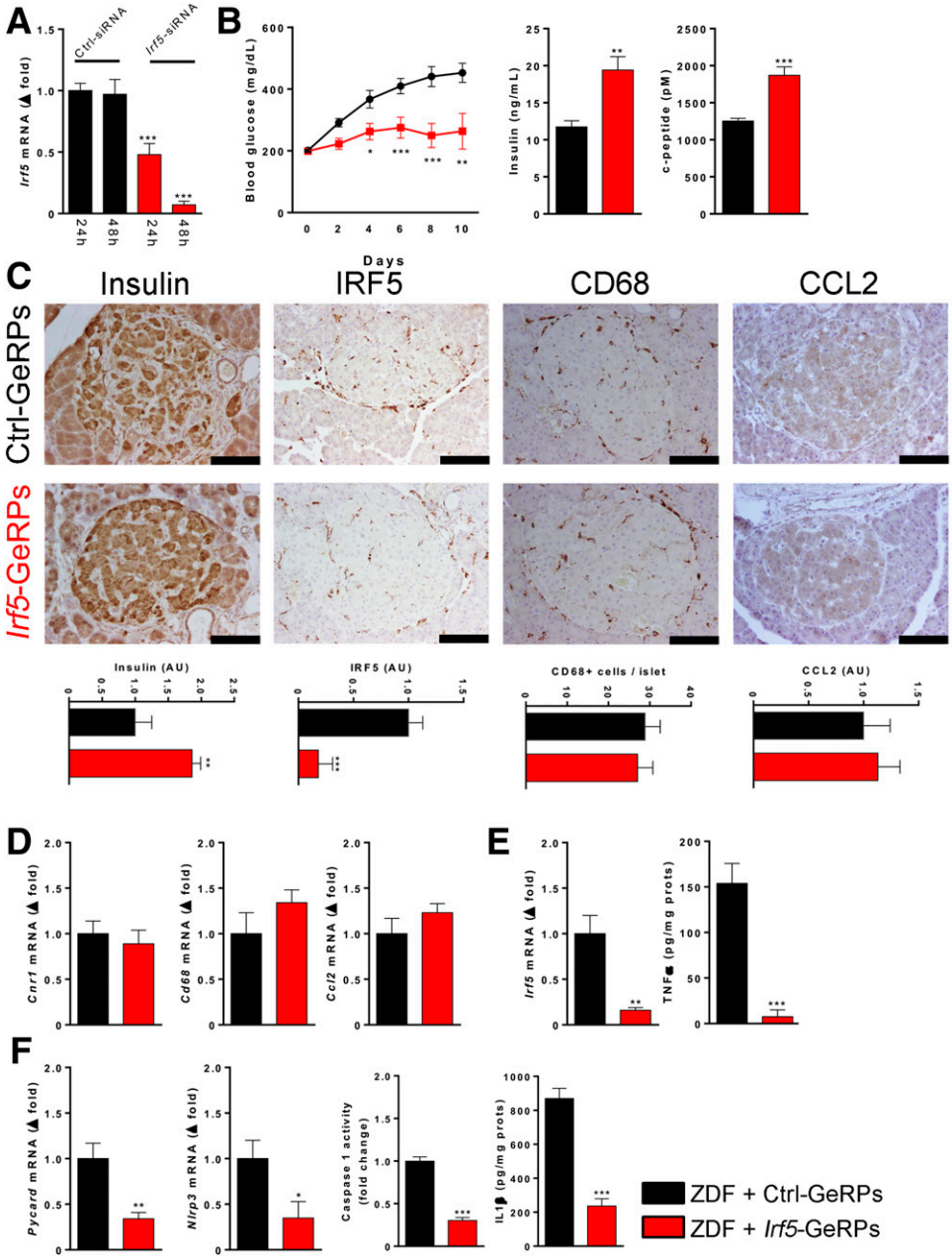

Figure 7—Effects of GeRP-mediated knockdown of *Irf5* in ZDF rats on islet protein and gene expression. *A*: In vitro validation in rat PECs of the *Irf5* siRNA used in vivo, as shown in panel *B*. *B*: GeRP-mediated delivery of Irf5 siRNA (red), but not control siRNA (black), protects ZDF rats from hyperglycemia and the loss of β-cell function. *C*: Representative immunohistological stainings for insulin, IRF5, CD68, and CCL2 protein levels in islets from ZDF rats treated with *Irf5* siRNA (red) vs. control siRNA (black). Scale bar, 100 μm. Quantitation by densitometry or immune-positive cell counts, as described in RESEARCH DESIGN AND METHODS. *D*: Lack of effect of in vivo knockdown of *Irf5* on *Cnr1*, *Cd68*, and *Ccl2* mRNA in isolated islets. *E*: Downregulation of *Irf5* expression and TNF-α protein in islets by the same treatment. *F*: Downregulation of *Pycard* and *Nlrp3* expression, caspase-1 activity, and IL-1β protein in islets of ZDF rats treated with *Irf5* siRNA vs. control siRNA-containing GeRPs. Points/columns and bars are mean ± SEM values from six rats/group. $^*P < 0.05$, $^{**}P < 0.01$, $^{***}P < 0.005$ relative to the control siRNA-treated group. AU, arbitrary unit.

for 12 days with GeRPs containing control siRNA or *Irf5* siRNA. ZDF rats treated with control siRNA developed progressive hyperglycemia, whereas those receiving *Irf5* siRNA maintained their pretreatment blood glucose level and also retained significantly higher plasma insulin and C-peptide levels (Fig. 7*B*). β-Cell protection was further indicated by the higher insulin content of islets from *Irf5* siRNA-treated rats compared with control siRNA-treated rats (Fig. 7*C*). As expected, *Irf5* knockdown significantly reduced Irf5 protein abundance in islets, whereas the number of $CD68^+$ macrophages and CCL2 protein levels were similar in the two groups, indicating a lack of IRF5

involvement in CCL2 secretion (Fig. 7*C*). Similarly, *Irf5* knockdown did not affect *Cnr1*, *CD68*, and *Ccl2* mRNA levels in islets (Fig. 7*D*) but resulted in a >90% decrease in TNF-α content (Fig. 7*E*), accompanied by significant decreases in *Pycard* and *Nlrp3* gene expression, caspase-1 activity, and IL-1β content (Fig. 7*F*). Furthermore, macrophage-specific in vivo knockdown of *Irf5* resulted in an increased in $CD3^+$ T lymphocytes (Supplementary Fig. 6*A*) associated with a decrease in T_H1 markers (Supplementary Fig. 6*B*) and an increase in T_H2 markers (Supplementary Fig. 6*C*), without a change in the T_H17 response (Supplementary Fig. 6*D*). Additionally, *Irf5* knockdown did not affect *Il12p40* or *Il23* expression but did increase *Il10* expression (Supplementary Fig. 6*E*).

DISCUSSION

Islet inflammation is a contributing factor to the progression of compensated IR into insulin-dependent T2D, and CB_1R on proinflammatory macrophages play a prominent role in diabetic insulitis and loss of β-cell function in the ZDF model of T2D (19). To test the developmental role of CB_1R in T2D, we generated CB_1R-deficient rats on a ZDF background. Here we report that ZDF-Cnr1 rats are as hyperinsulinemic and insulin resistant as ZDF rats, but they are protected from the loss of β-cell function and consequently remain normoglycemic and are also protected from the associated nephropathy. Furthermore, adoptive transfer of ZDF-Cnr1 BM to ZDF recipients replicates the preservation of β-cells and normoglycemia seen in ZDF-Cnr1 rats, but does not mitigate the loss of glomerular podocytes and the associated nephropathy. This provides strong evidence that CB_1Rs in BM-derived macrophages are both necessary and sufficient for the development of T2D but do not play a role in diabetic nephropathy in this model. Furthermore, we demonstrate for the first time the key role of IRF5, the master regulator of inflammatory polarization of macrophages (22), as a downstream signaling molecule mediating CB_1R-induced cytokine release by macrophages in vitro and the diabetogenic effect CB_1R activation in vivo.

ZDF-Cnr1 rats remain normoglycemic for up to 26 weeks of age and do not display the macrophage infiltration of islets and the associated loss of β-cell function observed in diabetic ZDF rats. The elevated levels of plasma FFA, TG, and total cholesterol, as well as the hypoadiponectemia are also normalized in ZDF-Cnr1 rats, which is in agreement with the documented role of CB_1R in these metabolic disturbances (17). Finally, ZDF-Cnr1 rats are protected from diabetic nephropathy, as reflected by normal parameters of renal function.

Interestingly, the hyperphagia of ZDF rats is also prevented by the knockout of *Cnr1*, indicating that the hyperphagia in leptin deficiency requires intact CB_1R signaling. The lower food intake of ZDF-Cnr1 rats was associated with a somewhat slower early weight gain (Fig. 1*D*), which could affect insulin sensitivity. However, *Cnr1* deletion protected β-cells and preserved β-cell function without affecting the IR of ZDF rats. Furthermore, adoptive transfer of CB_1R-deficient BM to ZDF rats prevented hyperglycemia and β-cell loss without affecting food intake or body weight (Fig. 4*D*). Thus, CB_1R-mediated effects on β-cell function are unrelated to changes in food intake or body weight.

The absence of hyperglycemia and β-cell loss in ZDF rats transplanted with $Cnr1^{-/-}$ BM is not due to the process of BMT per se, because transferring wild-type ZDF BM to wild-type ZDF recipients did not prevent the full development of hyperglycemia. The protective effect of $Cnr1^{-/-}$ BMT is reminiscent of the similar effect of macrophage-specific in vivo knockdown of *Cnr1* (19). The role of macrophage CB_1R in β-cell loss is further supported by the protective effect of macrophage-specific knockdown of *Irf5* and the regulation of *Irf5* expression by CB_1R. Thus, macrophage CB_1Rs are both necessary and sufficient to account for the development of T2D in this model. However, we cannot exclude the possibility that glucotoxicity and lipotoxicity (35) also contribute to β-cell damage, either directly or by inducing the EC/CB_1R system, as shown previously (19).

In contrast, the transfer of $Cnr1^{-/-}$ BM to ZDF rats did not mitigate diabetic nephropathy, indicating the involvement of a different cellular pool of CB_1Rs. This is in agreement with the absence of significant infiltration of proinflammatory macrophages into glomeruli during the development of nephropathy in ZDF rats (21). A similar lack of involvement of proinflammatory macrophages has been indicated by the findings that selective deletion of Nlrp3 or caspase-1 expression in BM-derived cells failed to protect mice against the development of diabetic nephropathy, and the protective effect of the global deletion of *Nlrp3* was not reversed by the transplantation of wild-type BM cells into *Nlrp3*-deficient mice (36).

The congruent effects of pharmacological blockade and genetic deletion of CB_1Rs strongly support the diabetogenic role of increased CB_1R activity. This is different from the situation in leptin-deficient *ob/ob* mice, in which germline deletion of *Cnr1* aggravated rather than mitigated their glucose intolerance (37). However, *ob/ob* mice on a C57BL/6J background compensate for IR by β-cell proliferation and thus do not become overtly diabetic, so the key pathogenic process promoted by CB_1R activity in ZDF rats was absent in the murine model. On the other hand, the deletion of *Cnr1* in both models failed to reverse basal hyperinsulinemia and IR, which is likely related to the leptin-deficient state. Leptin receptors are present on β-cells where they mediate increased K_{ATP} channel activity (38), and their activation was reported to decrease basal, but not glucose-stimulated, insulin secretion (39).

Most importantly, we discovered that the transcription factor IRF5 is a key downstream mediator of CB_1R-induced cytokine release by inflammatory macrophages and the resulting loss of β-cell function. First, *Irf5* expression was robustly increased in the islets of ZDF compared with lean control rats. This increase was prevented by pharmacological blockade or genetic deletion of CB_1R, which also prevented macrophage infiltration of islets,

suggesting that *Irf5* expression was induced in macrophages. This was then further confirmed by the CB_1R agonist–induced increase in *Irf5* expression in primary cultured mouse and rat macrophages or in THP-1 cells. This effect was PTX sensitive but unaffected by p38MAPK or JNK blockade or knockdown, suggesting that it resulted from $G_{i/o}$-mediated inhibition of adenylate cyclase. Furthermore, siRNA-mediated knockdown of *Irf5* in macrophages blunted the CB_1R agonist–induced increase in TNF-α and IL-1β secretion and *Nlrp3* expression, indicating the obligatory role of IRF5 in proinflammatory cytokine release. The anti-inflammatory response to *Irf5* knockdown also involved a T_H2-type immune response, as indicated by the increase in $CD3^+$ T lymphocytes and the increased expression of the T_H2 markers *Gata3* and *Il4* and decreased expression of the T_H1 marker *Tbet* in pancreatic islets. These changes are similar to those found in adipose tissue of mice with diet-induced obesity (23) and are consistent with the proposed role of a T_H1-type inflammatory response in T2D and its renal complications (40,41). Finally, macrophage-specific in vivo knockdown of *Irf5* in ZDF rats protected β-cells and prevented the development of hyperglycemia, similar to the earlier reported effects of chronic CB_1R blockade or selective knockdown of *Cnr1* in macrophages (19).

IRF5, originally discovered as a transcription factor induced by type I interferons during viral infections (42), was more recently identified as a master regulator of macrophage M1 polarization and a mediator of obesity-related adipose tissue inflammation and the resulting IR (23). The present findings establish that the G-protein–coupled receptor CB_1R is an upstream regulator of *Irf5* expression and point to a broader metabolic function of macrophage IRF5 as a key driver of diabetogenic insulitis and β-cell loss.

Unlike CB_1R blockade or gene deletion, which also reduced CCL2 chemokine secretion and the resulting transmigration of macrophages into islets (19), the knockdown of *Irf5* failed to influence these parameters. This suggested that CB_1Rs signal via an alternative, IRF5-independent pathway to promote CCL2 secretion. Indeed, CB_1R agonists activated p38MAPK and JNK but not ERK1/2 in rodent and human macrophages, and inhibitors of p38MAPK or JNK blocked the parallel increase in CCL2 secretion without affecting the increased secretion of TNF-α or IL-1β. The siRNA-mediated knockdown of p38MAPKα, but not p38MAPKβ, in THP-1 macrophages similarly inhibited CB_1R-induced CCL2, but not TNF-α secretion, and partially inhibited IL-1β secretion. This supports earlier findings that CB_1R promotes CCL2 secretion via p38MAPK (43), but documents for the first time show the selective role of the p38MAPKα isoform in this effect. Whereas the above findings indicate that inflammatory macrophages are an important source of CCL2, we could also detect this chemokine in β-cells, which is in agreement with evidence for CCL2 secretion by islet β-cells (31,32). It is possible that in the early stages of diabetic insulitis, β-cell–derived CCL2 initiates the transmigration of macrophages, which then amplify the production of this chemotactic signal. Another possible link between β-cells and macrophages is islet amyloid polypeptide, which is secreted by β-cells and stimulates inflammatory cytokine production by macrophages (44,45).

Together, the above findings demonstrate that activation of CB_1Rs in proinflammatory M1 macrophages increases chemokine and cytokine secretion via distinct, partially overlapping signaling pathways, as illustrated in Fig. 8. The

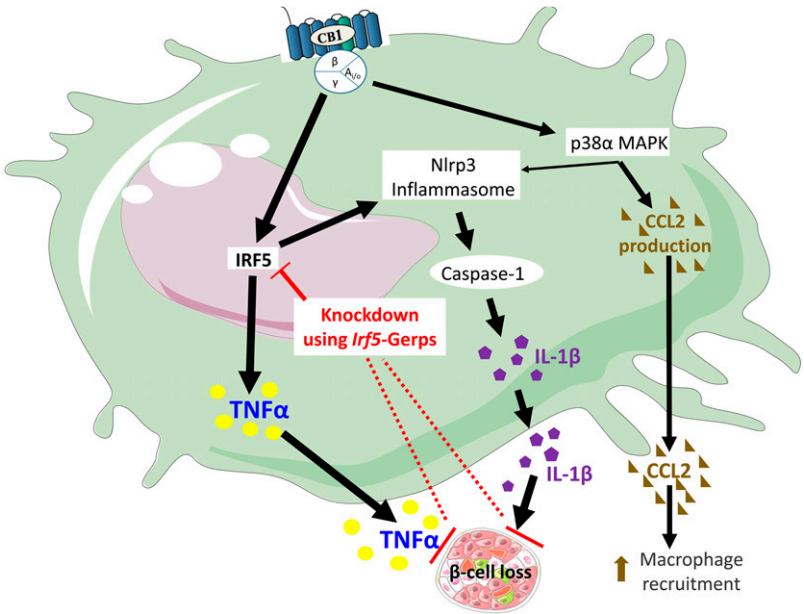

Figure 8—Schematic illustration of the proposed mechanism by which the activation of CB_1Rs in macrophages leads to the loss of β-cell function. This figure was prepared using a template on the Servier medical art website (http://www.servier.com/Powerpoint-image-bank).

CB_1R-induced secretion of CCL2, but not TNF-α, is mediated via the activation of p38MAPKα. On the other hand, the CB_1R-induced secretion of TNF-α, but not CCL2, is mediated via IRF5, and both pathways contribute to increased IL-1β secretion, with IRF5 having a more dominant role. The obligatory role of IRF5 in the secretion of cytotoxic cytokines thought to drive β-cell loss (19) is highlighted by the protective effect of macrophage-specific in vivo knockdown of *Irf5*. These findings mark IRF5 as a potential therapeutic target in T2D.

Acknowledgments. The authors thank J.F. McElroy and R.J. Chorvat (Jenrin Discovery) for providing the CB_1R antagonist JD5037, Peter Gao (National Institute on Alcohol Abuse and Alcoholism, National Institutes of Health [NIAAA, NIH]) for advice on whole-body irradiation and BM transplantation, Dan Pare (National Institute of Allergy and Infectious Diseases, NIH) for his help in performing whole-body irradiation, J. Harvey-White (NIAAA, NIH) for technical assistance, and R. Kechrid (NIAAA, NIH) for assistance with the animal studies.

Funding. G.S. is supported by a János Bólyai Research Scholarship of the Hungarian Academy of Sciences. The work from the laboratory of M.P.C. was supported by a grant from the NIH (DK-103047). This study was supported by intramural NIH funds to G.K.

Duality of Interest. No potential conflicts of interest relevant to this article were reported.

Author Contributions. T.J. designed the study, performed most of the experiments, designed and tested the GeRPs, analyzed the results, and wrote the manuscript. G.S. designed the study, performed Western blot analyses of macrophage signaling, analyzed the results, and wrote the manuscript. R.C. conducted radioligand binding assays. G.G. performed some of the whole-body irradiation and BM transfer experiments. D.J.H. conducted in vivo *Irf5*-silencing experiments. J.K.P. performed the morphometric analysis of adipocytes. S.N. prepared, provided, designed, and tested the GeRPs. Y.S. and M.P.C. prepared and provided the GeRPs. J.L. and Z.L. assisted with cell culture and PCR analyses. A.Z.R. performed the renal pathology analyses. G.K. designed the study, analyzed the results, and wrote the manuscript. All authors had access to the manuscript and agreed with the final version. G.K. is the guarantor of this work and, as such, had full access to all the data in the study and takes responsibility for the integrity of the data and the accuracy of the data analysis.

References

1. Muoio DM, Newgard CB. Mechanisms of disease: molecular and metabolic mechanisms of insulin resistance and beta-cell failure in type 2 diabetes. Nat Rev Mol Cell Biol 2008;9:193–205
2. Prentki M, Nolan CJ. Islet beta cell failure in type 2 diabetes. J Clin Invest 2006;116:1802–1812
3. Kahn SE. The relative contributions of insulin resistance and beta-cell dysfunction to the pathophysiology of Type 2 diabetes. Diabetologia 2003;46:3–19
4. Hirosumi J, Tuncman G, Chang L, et al. A central role for JNK in obesity and insulin resistance. Nature 2002;420:333–336
5. Ehses JA, Perren A, Eppler E, et al. Increased number of islet-associated macrophages in type 2 diabetes. Diabetes 2007;56:2356–2370
6. Pacher P, Bátkai S, Kunos G. The endocannabinoid system as an emerging target of pharmacotherapy. Pharmacol Rev 2006;58:389–462
7. Engeli S, Böhnke J, Feldpausch M, et al. Activation of the peripheral endocannabinoid system in human obesity. Diabetes 2005;54:2838–2843
8. Silvestri C, Di Marzo V. The endocannabinoid system in energy homeostasis and the etiopathology of metabolic disorders. Cell Metab 2013;17:475–490
9. Mazier W, Saucisse N, Gatta-Cherifi B, Cota D. The endocannabinoid system: pivotal orchestrator of obesity and metabolic disease. Trends Endocrinol Metab 2015;26:524–537
10. Després JP, Golay A, Sjöström L; Rimonabant in Obesity-Lipids Study Group. Effects of rimonabant on metabolic risk factors in overweight patients with dyslipidemia. N Engl J Med 2005;353:2121–2134
11. Scheen AJ, Finer N, Hollander P, Jensen MD, Van Gaal LF; RIO-Diabetes Study Group. Efficacy and tolerability of rimonabant in overweight or obese patients with type 2 diabetes: a randomised controlled study. Lancet 2006;368:1660–1672
12. O'Hare JD, Zielinski E, Cheng B, Scherer T, Buettner C. Central endocannabinoid signaling regulates hepatic glucose production and systemic lipolysis. Diabetes 2011;60:1055–1062
13. Furuya DT, Poletto AC, Freitas HS, Machado UF. Inhibition of cannabinoid CB1 receptor upregulates Slc2a4 expression via nuclear factor-κB and sterol regulatory element-binding protein-1 in adipocytes. J Mol Endocrinol 2012;49:97–106
14. Eckardt K, Sell H, Taube A, et al. Cannabinoid type 1 receptors in human skeletal muscle cells participate in the negative crosstalk between fat and muscle. Diabetologia 2009;52:664–674
15. Osei-Hyiaman D, Liu J, Zhou L, et al. Hepatic CB1 receptor is required for development of diet-induced steatosis, dyslipidemia, and insulin and leptin resistance in mice. J Clin Invest 2008;118:3160–3169
16. Miranville A, Herling AW, Biemer-Daub G, Voss MD. Reversal of inflammation-induced impairment of glucose uptake in adipocytes by direct effect of CB1 antagonism on adipose tissue macrophages. Obesity (Silver Spring) 2010;18:2247–2254
17. Tam J, Vemuri VK, Liu J, et al. Peripheral CB1 cannabinoid receptor blockade improves cardiometabolic risk in mouse models of obesity. J Clin Invest 2010;120:2953–2966
18. Tam J, Cinar R, Liu J, et al. Peripheral cannabinoid-1 receptor inverse agonism reduces obesity by reversing leptin resistance. Cell Metab 2012;16:167–179
19. Jourdan T, Godlewski G, Cinar R, et al. Activation of the Nlrp3 inflammasome in infiltrating macrophages by endocannabinoids mediates beta cell loss in type 2 diabetes. Nat Med 2013;19:1132–1140
20. Schäfer A, Pfrang J, Neumüller J, Fiedler S, Ertl G, Bauersachs J. The cannabinoid receptor-1 antagonist rimonabant inhibits platelet activation and reduces pro-inflammatory chemokines and leukocytes in Zucker rats. Br J Pharmacol 2008;154:1047–1054
21. Jourdan T, Szanda G, Rosenberg AZ, et al. Overactive cannabinoid 1 receptor in podocytes drives type 2 diabetic nephropathy. Proc Natl Acad Sci U S A 2014;111:E5420–E5428
22. Krausgruber T, Blazek K, Smallie T, et al. IRF5 promotes inflammatory macrophage polarization and TH1-TH17 responses. Nat Immunol 2011;12:231–238
23. Dalmas E, Toubal A, Alzaid F, et al. Irf5 deficiency in macrophages promotes beneficial adipose tissue expansion and insulin sensitivity during obesity. Nat Med 2015;21:610–618
24. Godlewski G, Jourdan T, Szanda G, et al. Mice lacking GPR3 receptors display late-onset obese phenotype due to impaired thermogenic function in brown adipose tissue. Sci Rep 2015;5:14953
25. Haffner SM, Miettinen H, Stern MP. The homeostasis model in the San Antonio Heart Study. Diabetes Care 1997;20:1087–1092
26. Iyer MR, Cinar R, Liu J, et al. Structural basis of species-dependent differential affinity of 6-alkoxy-5-aryl-3-pyridinecarboxamide cannabinoid-1 receptor antagonists. Mol Pharmacol 2015;88:238–244
27. Duran-Struuck R, Dysko RC. Principles of bone marrow transplantation (BMT): providing optimal veterinary and husbandry care to irradiated mice in BMT studies. J Am Assoc Lab Anim Sci 2009;48:11–22
28. Buehler E, Chen Y-C, Martin S. C911: a bench-level control for sequence specific siRNA off-target effects. PLoS One 2012;7:e51942
29. Tesz GJ, Aouadi M, Prot M, et al. Glucan particles for selective delivery of siRNA to phagocytic cells in mice. Biochem J 2011;436:351–362
30. Liu J, Zhou L, Xiong K, et al. Hepatic cannabinoid receptor-1 mediates diet-induced insulin resistance via inhibition of insulin signaling and clearance in mice. Gastroenterology 2012;142:1218–1228.e1

31. Piemonti L, Leone BE, Nano R, et al. Human pancreatic islets produce and secrete MCP-1/CCL2: relevance in human islet transplantation. Diabetes 2002; 51:55–65
32. Taylor-Fishwick DA, Weaver J, Glenn L, et al. Selective inhibition of 12-lipoxygenase protects islets and beta cells from inflammatory cytokine-mediated beta cell dysfunction. Diabetologia 2015;58:549–557
33. Sica A, Mantovani A. Macrophage plasticity and polarization: in vivo veritas. J Clin Invest 2012;122:787–795
34. Aouadi M, Tesz GJ, Nicoloro SM, et al. Orally delivered siRNA targeting macrophage Map4k4 suppresses systemic inflammation. Nature 2009;458: 1180–1184
35. Eguchi K, Manabe I, Oishi-Tanaka Y, et al. Saturated fatty acid and TLR signaling link β cell dysfunction and islet inflammation. Cell Metab 2012;15:518–533
36. Shahzad K, Bock F, Dong W, et al. Nlrp3-inflammasome activation in non-myeloid-derived cells aggravates diabetic nephropathy. Kidney Int 2015;87:74–84
37. Li Z, Schmidt SF, Friedman JM. Developmental role for endocannabinoid signaling in regulating glucose metabolism and growth. Diabetes 2013;62:2359–2367
38. Harvey J, McKenna F, Herson PS, Spanswick D, Ashford ML. Leptin activates ATP-sensitive potassium channels in the rat insulin-secreting cell line, CRI-G1. J Physiol 1997;504:527–535
39. Ishida K, Murakami T, Mizuno A, Iida M, Kuwajima M, Shima K. Leptin suppresses basal insulin secretion from rat pancreatic islets. Regul Pept 1997; 70:179–182
40. Zeng C, Shi X, Zhang B, et al. The imbalance of Th17/Th1/Tregs in patients with type 2 diabetes: relationship with metabolic factors and complications. J Mol Med (Berl) 2012;90:175–186
41. Zhang C, Xiao C, Wang P, et al. The alteration of Th1/Th2/Th17/Treg paradigm in patients with type 2 diabetes mellitus: relationship with diabetic nephropathy. Hum Immunol 2014;75:289–296
42. Barnes BJ, Moore PA, Pitha PM. Virus-specific activation of a novel interferon regulatory factor, IRF-5, results in the induction of distinct interferon alpha genes. J Biol Chem 2001;276:23382–23390
43. Han KH, Lim S, Ryu J, et al. CB1 and CB2 cannabinoid receptors differentially regulate the production of reactive oxygen species by macrophages. Cardiovasc Res 2009;84:378–386
44. Westwell-Roper C, Dai DL, Soukhatcheva G, et al. IL-1 blockade attenuates islet amyloid polypeptide-induced proinflammatory cytokine release and pancreatic islet graft dysfunction. J Immunol 2011;187:2755–2765
45. Masters SL, Dunne A, Subramanian SL, et al. Activation of the NLRP3 inflammasome by islet amyloid polypeptide provides a mechanism for enhanced IL-1β in type 2 diabetes. Nat Immunol 2010;11:897–904